

Cyclophilin A protects HIV-1 from restriction by human TRIM5 α

Kyusik Kim¹, Ann Dauphin¹, Sevnur Komurlu², Sean M. McCauley¹, Leonid Yurkovetskiy¹, Claudia Carbone¹, William E. Diehl¹, Caterina Strambio-De-Castillia¹, Edward M. Campbell^{2,3} and Jeremy Luban^{1,4*}

The HIV-1 capsid (CA) protein lattice encases viral genomic RNA and regulates steps essential to target-cell invasion¹. Cyclophilin A (CypA) has interacted with the CA of lentiviruses related to HIV-1 for millions of years²⁻⁷. Disruption of the CA–CypA interaction decreases HIV-1 infectivity in human cells⁸⁻¹² but stimulates infectivity in non-human primate cells¹³⁻¹⁵. Genetic and biochemical data suggest that CypA protects HIV-1 from a CA-specific restriction factor in human cells¹⁶⁻²⁰. Discovery of the CA-specific restriction factor tripartite-containing motif 5 α (TRIM5 α)²¹ and multiple, independently derived, TRIM5–CypA fusion genes^{4,5,15,22-26} pointed to human TRIM5 α being the CypA-sensitive restriction factor. However, HIV-1 restriction by human TRIM5 α in tumour cell lines is minimal²¹ and inhibition of such activity by CypA has not been detected²⁷. Here, by exploiting reverse genetic tools optimized for primary human blood cells, we demonstrate that disruption of the CA–CypA interaction renders HIV-1 susceptible to potent restriction by human TRIM5 α , with the block occurring before reverse transcription. Endogenous TRIM5 α associated with virion cores as they entered the cytoplasm, but only when the CA–CypA interaction was disrupted. These experiments resolve the long-standing mystery of the role of CypA in HIV-1 replication by demonstrating that this ubiquitous cellular protein shields HIV-1 from previously inapparent restriction by human TRIM5 α .

To assess the role of TRIM5 α and CypA in the primary human blood cell types that serve as targets for HIV-1 infection in vivo, lentiviral vectors were optimized for titre and knockdown efficiency in these cells²⁷⁻³¹. Primary human macrophages, dendritic cells and CD4⁺ T cells were transduced with lentivectors bearing a puromycin resistance cassette and short hairpin RNAs (shRNAs) targeting either TRIM5 or luciferase (Luc) as a control. After three days of selection in puromycin, knockdown was confirmed by quantitative PCR with reverse transcription (RT–qPCR) for TRIM5 mRNA and by rescue of N-tropic murine leukemia virus restriction (Extended Data Fig. 2a–c), as done previously^{27,28}. TRIM5 and Luc control knockdown cells were then challenged with single-cycle, vesicular stomatitis virus glycoprotein (VSV G)-pseudotyped, HIV-1–green fluorescent protein (GFP) reporter vectors. Three days later, the percentage of GFP⁺ cells was assessed by flow cytometry as a measure of infectivity (see Extended Data Fig. 1 for the gating strategy).

Compared to Luc control knockdown, TRIM5 knockdown had minimal effect on wild-type (WT) HIV-1 transduction efficiency in

macrophages, dendritic cells or CD4⁺ T cells (Fig. 1a–d; Extended Data Fig. 3a). The infectivity of HIV-1 CA-P90A, a mutant that disrupts CypA binding^{8,9}, was attenuated compared to the WT in control knockdown cells generated with all three cell types (Fig. 1a–d). The effect was evident in cells from all blood donors tested (at least three blood donors per condition) and over a 100-fold range in challenge vector titre (Extended Data Fig. 3a). TRIM5 knockdown in macrophages, dendritic cells or CD4⁺ T cells increased CA-P90A infectivity (Fig. 1a–d; Extended Data Fig. 3a). Results were the same whether the challenge was with a three-plasmid vector system based on the clade B HIV-1_{NL4-3} lab strain^{30,32} (Fig. 1a–c) or a two-plasmid vector system based on the clade C HIV-1_{ZM249M} transmission-founder strain from Zambia^{30,33} (Fig. 1d).

Given previous reports that endogenous human TRIM5 α in immortalized cell lines has a modest effect on HIV-1 infectivity, and that CypA and TRIM5 α act independently to regulate HIV-1 transduction²⁷, the relatively large magnitude rescue of CA-P90A infectivity by TRIM5 knockdown in primary human blood cells was surprising. Complementary pharmacologic and reverse genetic approaches were therefore used to disrupt the CA–CypA interaction. For pharmacologic disruption, cells were incubated in media containing small molecules that compete with CA for binding to CypA^{2,8-10,34}. Compared to dimethylsulfoxide (DMSO) solvent alone, cyclosporine A (CsA) reduced HIV-1 transduction efficiency in Luc control knockdown macrophages (Fig. 1e). In contrast, cyclosporine H (CsH), an analogue with 1,000-fold lower affinity for CypA³⁵, caused only a slight increase in HIV-1 infection (Extended Data Fig. 3b). Since CsA blocks T cell proliferation, two non-immunosuppressive CypA inhibitors derived from sanglifehrin A, GS–CypAi3 and GS–CypAi48 (ref. ³⁴), were used instead on this cell type; these drugs decreased HIV-1 transduction efficiency in primary CD4⁺ T cells (Fig. 1f; Extended Data Fig. 3c–e). TRIM5 knockdown reversed the HIV-1 inhibition in macrophages caused by CsA (Fig. 1e), or in CD4⁺ T cells caused by the sanglifehrin A-derivatives (Fig. 1f; Extended Data Fig. 3c–e).

To disrupt the CA–CypA interaction using a genetic approach, macrophages were transduced with two vectors for the knockdown of either TRIM5 or CypA, or both. The first vector conferred puromycin resistance and expressed shRNAs targeting either TRIM5 or Luc. The second vector conferred blasticidin resistance and expressed shRNAs targeting either CypA or Luc. After simultaneous transduction with pairs of these vectors, macrophages were selected for three days in both puromycin and blasticidin and then

¹Program in Molecular Medicine, University of Massachusetts Medical School, Worcester, MA, USA. ²Department of Microbiology and Immunology, Stritch School of Medicine, Loyola University Chicago, Maywood, IL, USA. ³Infectious Disease and Immunology Institute, Stritch School of Medicine, Loyola University Chicago, Maywood, IL, USA. ⁴Department of Biochemistry and Molecular Pharmacology, University of Massachusetts Medical School, Worcester, MA, USA. *e-mail: jeremy.luban@umassmed.edu

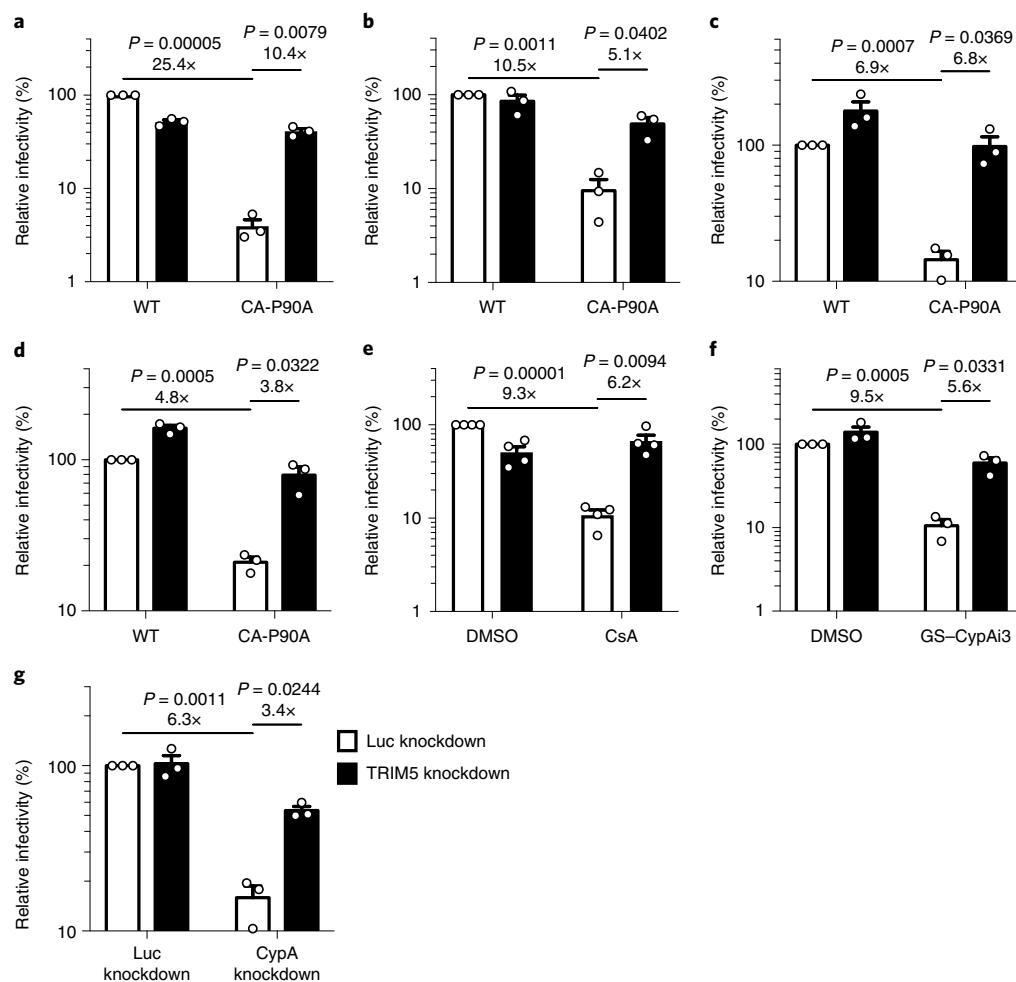


Fig. 1 | Disruption of the CA–CypA interaction in primary human blood cells renders HIV-1 susceptible to restriction by TRIM5. a–d, Macrophages (a), dendritic cells (b) or CD4⁺ T cells (c,d) were selected after transduction with a lentivirus expressing shRNA targeting TRIM5 or Luc (control) and challenged with single-cycle, VSV G-pseudotyped, HIV-1_{NL4-3}–GFP (a–c) or HIV-1_{ZM249M}–GFP (d), bearing WT CA or CA-P90A (mean \pm s.e.m., $n=3$ donors for each). e, TRIM5 knockdown or Luc knockdown macrophages were challenged with HIV-1_{NL4-3}–GFP in the presence of 8 μ M CsA or DMSO solvent (mean \pm s.e.m., $n=4$ donors). f, TRIM5 knockdown or Luc knockdown CD4⁺ T cells were challenged with HIV-1_{ZM249M}–GFP in the presence of 2.5 μ M GS–CypAi3 or DMSO solvent (mean \pm s.e.m., $n=3$ donors). g, Macrophages were transduced simultaneously with two vectors expressing shRNAs, as indicated, and selected with puromycin and blasticidin. Cells were then challenged with HIV-1_{NL4-3}–GFP (mean \pm s.e.m., $n=3$ donors). The percentage of GFP⁺ cells was assessed by flow cytometry and normalized to the WT in Luc control knockdown cells in all cases. Significance was determined by two-tailed, paired Student's *t*-test.

challenged with single-cycle, VSV G-pseudotyped, HIV-1–GFP reporter vector bearing WT CA. Compared to the Luc control knockdown, CypA knockdown reduced CypA protein levels ~70% (Extended Data Fig. 2d). As with CA-P90A and the small molecule inhibitors, CypA knockdown decreased transduction efficiency (Fig. 1g). This effect was rescued by simultaneous knockdown of TRIM5 (Fig. 1g) without restoring CypA protein levels (Extended Data Fig. 2d). Taken together, these data indicate that endogenous human TRIM5 is required for HIV-1 restriction in the absence of the CA–CypA interaction. Consistent with the previously reported CA-specific saturation of TRIM5 restriction activity^{13,27}, the effective titre of HIV-1–GFP reporter vector bearing CA-P90A was increased in a dose-dependent manner by the addition of virus-like particles (VLPs) bearing CA-P90A, but not by VLPs bearing WT CA (Extended Data Fig. 4).

Although the shRNA that targets TRIM5 is distinguished from the next most similar sequence in the human genome (GRCh38) by multiple mismatches, off-target effects are theoretically possible. To test whether TRIM5 α is sufficient to explain the HIV-1 restriction

activity associated with CA–CypA disruption, a vector was designed based on the ubiquitin fusion technique³⁶ that expresses a tripartite fusion of puromycin *N*-acetyl transferase (Puro^R), the K48R mutant of ubiquitin (Ub^{K48R}) and the coding sequence for a protein of interest, in addition to an shRNA (Fig. 2a). Four variants of the plasmid were engineered in which the shRNA targeted either TRIM5 or Luc, with or without a TRIM5 α coding sequence bearing mismatches in the shRNA target sequence (Fig. 2a).

Macrophages (Fig. 2b) and CD4⁺ T cells (Fig. 2c) were transduced with each of the four variants of the shRNA tripartite fusion vector and selected for three days with puromycin. Cells were then challenged with the three-plasmid HIV-1–GFP reporter vector used in Fig. 1a–c and assessed by flow cytometry for percentage of GFP⁺ cells three days later. As in Fig. 1, the infectivity of the vector bearing WT CA was minimally affected by TRIM5 knockdown or by TRIM5 α overexpression (Fig. 2b,c). Compared to the WT, the infectivity of vector bearing CA-P90A was decreased (Fig. 2b,c) and the infectivity of this mutant was rescued by TRIM5 shRNA (Fig. 2b,c). In the presence of shRNA targeting TRIM5, delivery of

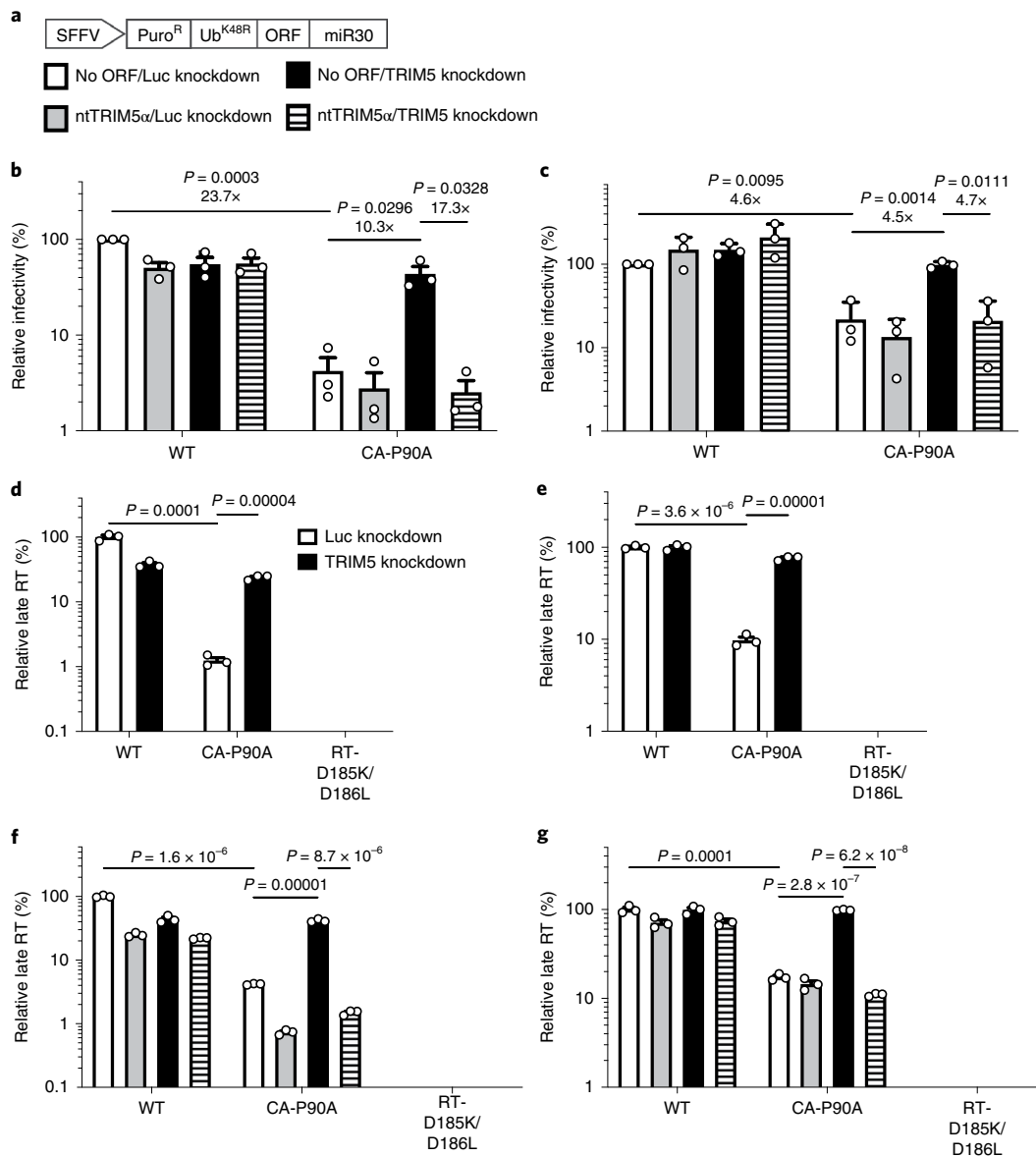


Fig. 2 | Human TRIM5 α is sufficient to explain the inhibition of reverse transcription that results from disruption of CA–CypA interaction. **a**, A schematic representation of an all-in-one shRNA-rescue lentivector, in which the spleen focus-forming virus (SFFV) promoter expresses a tripartite fusion of Puro^R, Ub^{K48R} and an open reading frame (ORF) for a gene of interest, as well as a microRNA30-based shRNA (miR30). **b,c**, All-in-one lentivectors encoding empty control (no ORF) or non-targetable, shRNA-resistant TRIM5 α coding sequence (ntTRIM5 α), along with shRNA targeting Luc or TRIM5, as indicated in **a**, were used to transduce macrophages (**b**) or CD4⁺ T cells (**c**). The percentage of GFP-expressing cells was measured by flow cytometry and normalized to the values for no ORF/Luc knockdown cells challenged with WT CA; mean \pm s.e.m., $n = 3$ donors for each. Significance was determined by two-tailed, paired Student's *t*-test. **d–g**, TRIM5 knockdown or Luc knockdown macrophages (**d**) or CD4⁺ T cells (**e**), macrophages (**f**) or CD4⁺ T cells (**g**) transduced with the all-in-one shRNA-rescue lentivectors described in **a** were challenged with HIV-1_{NL4-3}–GFP containing WT CA or CA-P90A, as indicated. DNA was extracted 20 h post challenge and late products of reverse transcription were assessed by qPCR (mean \pm s.e.m., $n = 3$ biologically independent samples). RT-D185K/D186L mutant virus was used as a control for background signal. Significance was determined by two-tailed, unpaired Student's *t*-test.

TRIM5 α coding sequence bearing shRNA target-site mismatches restored restriction activity to the control level (Fig. 2b,c). These results demonstrate that, in primary human blood cells, human TRIM5 α is sufficient to restrict HIV-1 transduction, but only when the CA–CypA interaction is disrupted.

To determine at which step in the virus life cycle human TRIM5 α inhibits HIV-1 when the CA–CypA interaction is disrupted, HIV-1 complementary DNA (cDNA) resulting from reverse transcription was assessed by qPCR. Macrophages and CD4⁺ T cells were stably transduced and selected with vector expressing shRNAs targeting

TRIM5 or Luc (control) (Fig. 2d,e), or with each of the four variants of the shRNA tripartite fusion vector (Fig. 2f,g). Cells were then challenged with a HIV-1 reporter vector that had the 34 base pair loxP sequence in the U3 region of the 3' long terminal repeat to distinguish reporter vector transcripts from those of the shRNA lentivector³⁷. DNA was collected 20 h post challenge and qPCR was performed using primers specific for full-length linear HIV-1 cDNA (late RT). In all experiments, reporter vector bearing the RT-D185K/D186L loss-of-function mutation³⁷ was included as a control for background signal not due to nascent reverse transcription (Fig. 2d–g).

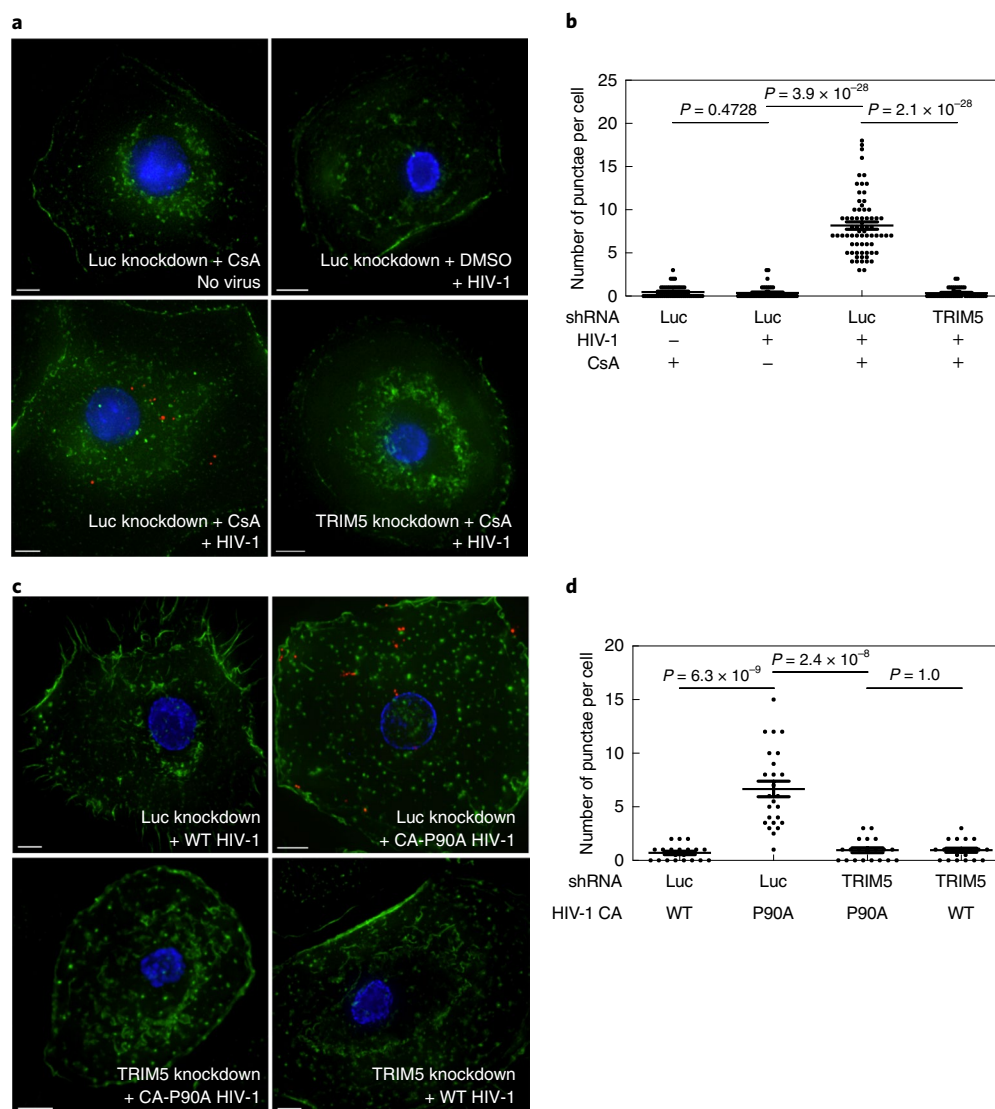


Fig. 3 | Endogenous TRIM5 α in primary human macrophages associates with HIV-1 CA after acute challenge but only when the CA–CypA interaction is disrupted. **a–d**, Macrophages were transduced and selected with vector bearing shRNA targeting either TRIM5 or Luc. Cells were then challenged for 2 h with VSV G-pseudotyped HIV-1_{NL4-3}–GFP in the presence of 5 μ M CsA or DMSO solvent (**a,b**) or challenged with HIV-1_{NL4-3}–GFP harbouring WT CA or CA-P90A (**c,d**), as indicated. Cells were fixed and PLA was performed with antibodies against HIV-1 CA and TRIM5 α . The representative images in **a,c** show PLA punctae (red), nuclei stained with Hoechst (blue) and actin filaments stained with phalloidin (green). The graphs in **b,d** show the number of PLA punctae per cell with mean \pm s.e.m. For **b**: Luc knockdown + CsA, no virus, $n = 45$ cells analysed; Luc knockdown + DMSO + HIV-1, $n = 45$; Luc knockdown + CsA + HIV-1, $n = 69$; TRIM5 knockdown + CsA + HIV-1, $n = 45$. For **d**: Luc knockdown + WT HIV-1, $n = 20$; Luc knockdown + CA-P90A HIV-1, $n = 25$; TRIM5 knockdown + CA-P90A HIV-1, $n = 20$; TRIM5 knockdown + WT HIV-1, $n = 20$. Significance was determined by two-tailed, unpaired Student's *t*-test. The data shown are representative of four independent experiments using cells from four blood donors for each condition. Scale bars in **a** and **c**, 5 μ m.

In Luc control knockdown macrophages and CD4⁺ T cells, viral cDNA was reduced by CA-P90A and this reduction was reversed by TRIM5 knockdown (Fig. 2d,e). Viral cDNA was also reduced by CA-P90A in either cell type transduced with the control shRNA tripartite fusion vector (Fig. 2f,g). TRIM5 shRNA rescued the cDNA (Fig. 2d–g) and rescue of TRIM5 α with the non-targetable coding sequence again decreased the CA-P90A cDNA (Fig. 2f,g). These results demonstrate that, when the CA–CypA interaction is disrupted, human TRIM5 α blocks HIV-1 at an early step of viral infection, before the completion of reverse transcription.

To determine whether TRIM5 α associates with HIV-1 CA in cells when the CA–CypA interaction is disrupted, primary human macrophages were stably transduced with TRIM5 shRNA or Luc shRNA and then challenged for 2 h with WT HIV-1 reporter vector

in the presence or absence of CsA, or with HIV-1 vectors bearing WT CA or CA-P90A. Cells were fixed and subjected to the proximity ligation assay (PLA) with antibodies specific for HIV-1 CA and endogenous human TRIM5 α . When cells were challenged with WT HIV-1 in the absence of CsA, very few punctae were detected (Fig. 3a–d; Extended Data Fig. 5a–d). Similarly, few punctae were detected when cells were treated with CsA in the absence of HIV-1 challenge (Fig. 3a,b; Extended Data Fig. 5a,b). By contrast, when cells were challenged with WT HIV-1 in the presence of CsA or with HIV-1 CA-P90A, multiple punctae were detected (Fig. 3a–d; Extended Data Fig. 5a–d), an increase of at least 10- and 20-fold in the average number of punctae per cell over the background, respectively (Fig. 3b,d; Extended Data Fig. 5b,d). TRIM5 knockdown eliminated the punctae (Fig. 3a–d; Extended Data Fig. 5a–d);

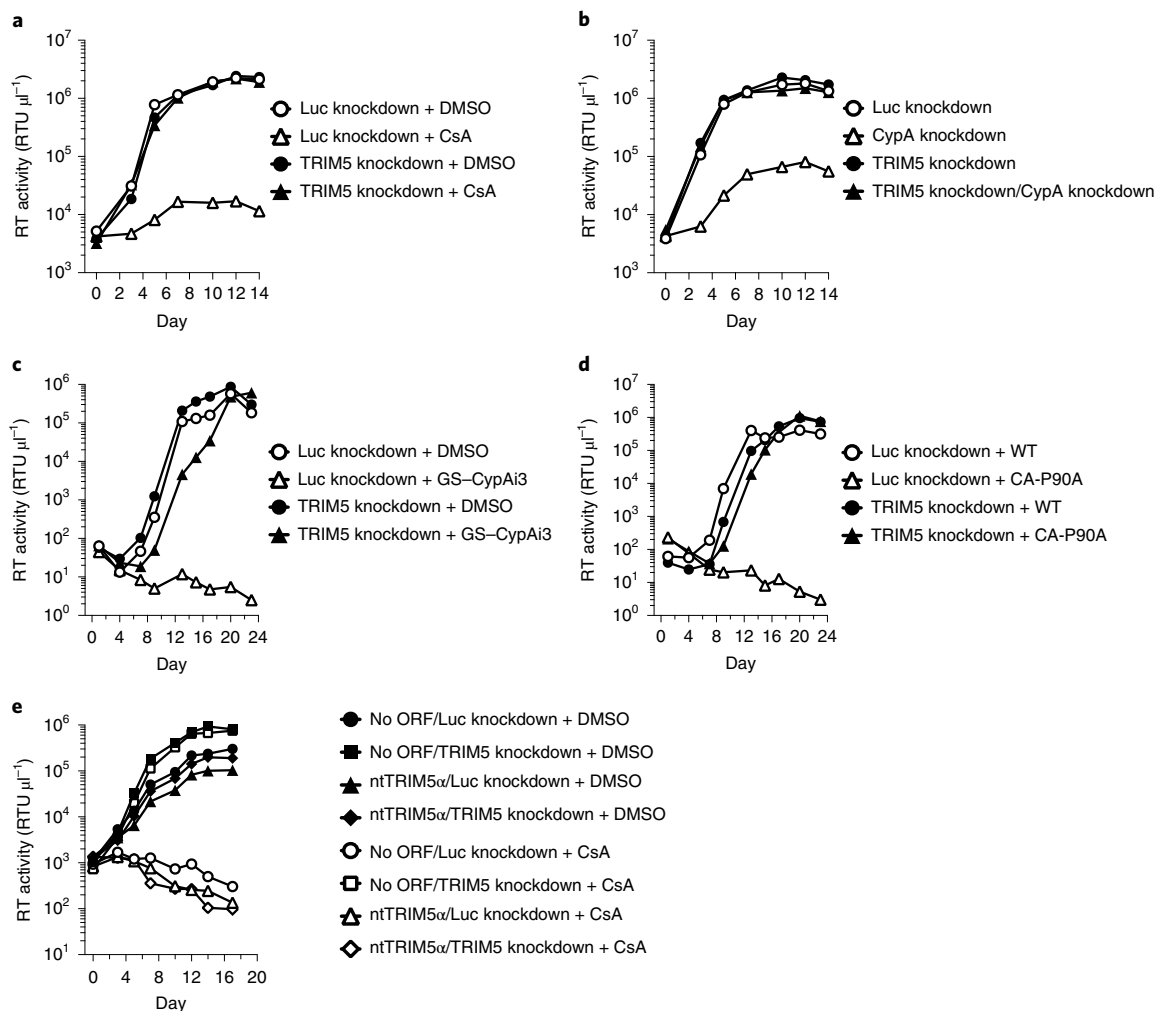


Fig. 4 | Endogenous TRIM5 α suppresses the spread of HIV-1 infection in primary human macrophages and CD4⁺ T cells when the CA–CypA interaction is disrupted. **a,b**, The spread of HIV-1_{MAC} infection in TRIM5 or Luc knockdown macrophages with 5 μ M CsA (**a**) or with vectors bearing shRNAs targeting CypA or Luc (**b**), as indicated. **c,d**, The spread of HIV-1_{ZM249M} infection in CD4⁺ T cells expressing shRNA targeting TRIM5 or Luc with 2.5 μ M GS–CypAi3 (**c**) or when challenged with virus bearing CA-P90A (**d**), as indicated. **e**, The spread of HIV-1_{MAC} infection in macrophages transduced with the all-in-one shRNA-rescue lentivectors described in Fig. 2, as indicated. HIV-1 replication was monitored by measuring reverse transcriptase activity (RTU μ l⁻¹) in the culture supernatant over time. The data shown are representative of two independent experiments using cells from two blood donors for each condition.

this indicated that the PLA signal was dependent on TRIM5 expression. The PLA signal was also dependent on the proteasome inhibitor MG132 (Extended Data Fig. 6), a result consistent with the reported involvement of the proteasome in the inhibition of reverse transcription by TRIM5 α ³⁸. These results indicate that, in the infection of primary human cells, endogenous TRIM5 α associates with HIV-1 CA when the CA–CypA interaction is disrupted.

The above experiments used single-cycle HIV-1 vectors. The effect of CypA on HIV-1 restriction by human TRIM5 α was therefore evaluated next using replication-competent HIV-1 in a context where the virus spreads from cell to cell. Primary human macrophages were challenged with clade B HIV-1 bearing a macrophage-tropic *env* (HIV-1_{MAC}) and replication was monitored for 14 days by measuring the accumulation of reverse transcriptase activity in the supernatant. As in the single-cycle experiments (Fig. 1), TRIM5 knockdown itself had little effect on WT HIV-1 replication (Fig. 4a,b). Disruption of the CA–CypA interaction with CsA (Fig. 4a) or with shRNA targeting CypA (Fig. 4b) effectively suppressed viral spread in the culture and, in both cases, replication kinetics were completely restored to the control level by shRNA targeting TRIM5 (Fig. 4a,b). Primary CD4⁺ T cells were then challenged

with a clade C transmission-founder virus (HIV-1_{ZM249M}). As observed in macrophages, TRIM5 knockdown alone had minimal effect on WT HIV-1 replication (Fig. 4c,d). No viral replication was detectable when the CA–CypA interaction was disrupted by the small molecule GS–CypAi3 (Fig. 4c) or by the presence of CA-P90A in HIV-1 (Fig. 4d); in both cases shRNA targeting TRIM5 rescued replication kinetics to the level of the controls (Fig. 4c,d). Furthermore, the shRNA tripartite fusion vectors were exploited to rule out off-target effects of the shRNA and to demonstrate that TRIM5 α is sufficient to restrict HIV-1 replication under conditions in which the CA–CypA interaction is interrupted (Fig. 4e).

The experiments presented here demonstrate that, in primary human blood cells, HIV-1 exploits CypA to evade CA recognition by, and the antiviral activity of, endogenous TRIM5 α . The simplest model is that CypA sterically blocks TRIM5 α from binding to CA. Alternatively, since CypA possesses peptidyl-prolyl isomerase activity³⁹ and HIV-1 CA-P90 is a validated substrate⁴⁰, CypA might shift the CA conformation and thereby protect HIV-1 CA from recognition by TRIM5 α . This answers the long-standing question of how CypA promotes HIV-1 infection and clearly establishes that, in the absence of CypA, human TRIM5 α potentially restricts HIV-1.

Conservation of the lentiviral CA–CypA interaction across millions of years of evolution is probably a result of selective pressure applied by TRIM5 orthologues encoded by host species that are otherwise permissive for lentiviral replication. In contrast to the results here, the observation that CypA promotes restriction in non-human primate cells^{13–15} probably reflects a different mode of CA recognition by TRIM5 α orthologues from these species. Finally, the results here indicate that, by rendering HIV-1 susceptible to the potent antiviral activity of TRIM5 α , non-immunosuppressive CypA inhibitors have the potential to make an important contribution to anti-HIV-1 drug cocktails.

Methods

Plasmids. All the plasmids used here are described in Supplementary Table 1 and are available, along with full sequences, at https://www.addgene.org/Jeremy_Luban/.

Human blood. Leukopaks were obtained from anonymous, healthy blood donors (New York Biologics). These experiments were reviewed by the University of Massachusetts Medical School Institutional Review Board and declared to be non-human subjects research, according to National Institutes of Health (NIH) guidelines (http://grants.nih.gov/grants/policy/hs/faqs_aps_definitions.htm).

Cell culture. All cells were cultured in humidified, 5% CO₂ incubators at 37 °C. HEK293 cells (American Type Culture Collection) were cultured in DMEM supplemented with 10% heat-inactivated FBS, 1 mM sodium pyruvate, 20 mM GlutaMAX-I, 1 \times MEM non-essential amino acids and 25 mM HEPES, pH 7.2 (DMEM–FBS complete). Peripheral blood mononuclear cells (PBMCs) were isolated from leukopaks by gradient centrifugation on Lymphoprep (Axis-Shield Poc AS, catalogue no. AXS-1114546). To generate dendritic cells or macrophages, CD14⁺ mononuclear cells were enriched by positive selection using anti-CD14 antibody microbeads (Miltenyi, catalogue no. 130-050-201). Enriched CD14⁺ cells were plated in RPMI-1640, supplemented with 5% heat-inactivated human AB⁺ serum (Omega Scientific), 1 mM sodium pyruvate, 20 mM GlutaMAX-I, 1 \times MEM non-essential amino acids and 25 mM HEPES, pH 7.2 (RPMI–HS complete), at a density of 10⁶ cells ml⁻¹ for macrophages or 2 \times 10⁶ cells ml⁻¹ for dendritic cells. To differentiate CD14⁺ cells into macrophages, 1:100 human granulocyte–macrophage colony stimulating factor (hGM-CSF)-conditioned media was added. To differentiate CD14⁺ cells into dendritic cells, 1:100 cytokine-conditioned media containing hGM-CSF and human interleukin-4 (hIL-4) was added. hGM-CSF and hIL-4 were produced from HEK293 cells transfected with pAIP-hGMCSF-co (Addgene no. 74168) or pAIP-hIL4-co (Addgene no. 74169), as previously described^{28,30}. CD4⁺ T cells were isolated from CD14-depleted PBMCs using anti-CD4 antibody microbeads (Miltenyi, catalogue no. 130-045-101); enrichment was typically >90%, as assessed by measuring the percentage of CD3⁺/CD4⁺ cells via flow cytometry with fluorescein isothiocyanate (FITC)-anti-CD3 (Biolegend, catalogue no. 317306) and allophycocyanin (APC)-anti-CD4 (Biolegend, catalogue no. 317416). The cells were cultured in RPMI-1640 supplemented with 10% heat-inactivated FBS, 1 mM sodium pyruvate, 20 mM GlutaMAX-I, 1 \times MEM non-essential amino acids and 25 mM HEPES, pH 7.2 (RPMI–FBS complete) with 50 U ml⁻¹ hIL-2 (NIH AIDS Reagent Program, catalogue no. 136).

Virus production. 24 h before transfection, 6 \times 10⁵ HEK293 cells were plated per well in six-well plates. All transfections used 2.49 μ g plasmid DNA with 6.25 μ l TransIT LT1 transfection reagent (Mirus) in 250 μ l Opti-MEM (Gibco). 2.49 μ g of replication-competent HIV-1 provirus DNA was transfected. For two-part, single-cycle vector, or for HIV-1 VLPs lacking a packageable genome, 2.18 μ g of *env*-defective HIV-1 provirus or p8.9 Δ SB *gag-pol* plasmid was cotransfected with 0.31 μ g pMD2.G VSV G plasmid, respectively. Three-part, single-cycle vectors were produced by cotransfecting 1.25 μ g minimal lentivector genome plasmid (pALPS-GFP, pWPTS-GFP, pLXIN-GFP, pAPM-D4-miR30, pABM-D4-miR30 or pPU-ORF-miR30), 0.93 μ g *gag-pol* plasmid (psPAX2, p8.9 Δ SB, pCIG3-N or pCIG3-B⁴¹) and 0.31 μ g pMD2.G VSV G plasmid. Vpx-containing simian immunodeficiency virus (SIV)–VLPs were produced by the transfection of 2.18 μ g pSIV3+ and 0.31 μ g pMD2.G plasmid. 16 h post transfection, the culture media was changed to the media specific for the cells to be transduced. Viral supernatant was harvested at 72 h, passed through a 0.45 μ m filter and stored at –80 °C.

Exogenous reverse transcriptase assay. A total of 5 μ l transfection supernatant was mixed with 5 μ l 0.25% Triton X-100, 50 mM KCl, 100 mM Tris–HCl pH 7.4 and 0.4 U μ l⁻¹ RiboLock RNase inhibitor and then diluted 1:100 in 5 mM (NH₄)₂SO₄, 20 mM KCl and 20 mM Tris–HCl pH 8.3. 10 μ l of this was then added to a single-step, RT–PCR assay with 35 nM bacteriophage MS2 RNA (Integrated DNA Technologies) as a template, 500 nM of each primer (5′-TCCTGCTCAACTTCCTGTCGAG-3′ and 5′-CACAGGTCAAACCTCTAGGAATG-3′) and 0.1 μ l hot-start Taq DNA polymerase (Promega) in 20 mM Tris–HCl pH 8.3, 5 mM (NH₄)₂SO₄, 20 mM KCl, 5 mM MgCl₂, 0.1 mg ml⁻¹ BSA, 1/20,000 SYBR Green I (Invitrogen)

and 200 μ M of deoxynucleotides (dNTPs) in a total reaction volume of 20 μ l. The RT–PCR reaction was carried out in a Bio-Rad CFX96 real-time PCR detection system with the following parameters: 42 °C for 20 min, 95 °C for 2 min and 40 cycles (95 °C for 5 s, 60 °C for 5 s, 72 °C for 15 s and acquisition at 80 °C for 5 s).

Transduction with lentiviral knockdown vectors. For dendritic cells, 2 \times 10⁶ CD14⁺ monocytes ml⁻¹ were transduced with a 1:4 volume of SIV–VLPs and a 1:4 volume of knockdown lentivector. For macrophages, 10⁶ CD14⁺ monocytes ml⁻¹ were transduced with a 1:8 volume of SIV–VLPs and a 1:8 volume of knockdown lentivector. The Vpx-containing SIV–VLPs were added to these cultures to overcome a SAMHD1 block to lentiviral transduction^{42,43}. Transduced cells were selected with 3 μ g ml⁻¹ puromycin (InvivoGen, catalogue no. ant-pr-1), 10 μ g ml⁻¹ blasticidin (InvivoGen, catalogue no. ant-bl-1) or both, for 3 d, starting 3 d post transduction.

Following isolation with magnetic beads, human CD4⁺ T cells were cultured at 2 to 3 \times 10⁶ cells ml⁻¹ in RPMI–FBS complete, supplemented with 50 U ml⁻¹ hIL-2 and stimulated with 5 μ g ml⁻¹ PHA-P (Sigma-Aldrich, catalogue no. L-1668). Alternatively, CD4⁺ T cells at 10⁶ cells ml⁻¹ were stimulated with 25 μ l ml⁻¹ ImmunoCult Human CD3/CD28 T Cell Activator (STEMCELL Technologies, catalogue no. 10991). At day 3 post stimulation, T cells were replated at 2 to 3 \times 10⁶ cells ml⁻¹ in RPMI–FBS complete, with 50 U ml⁻¹ hIL-2. Cells were transduced with 10⁵ reverse transcription units (RTUs) of viral vector per 10⁶ cells for 3 d, followed by selection with 2 μ g ml⁻¹ puromycin. After selection for 3 d, cells were restimulated with PHA-P or ImmunoCult Human CD3/CD28 T Cell Activator for 3 d. The stimulated cells were then replated at 2 to 3 \times 10⁶ cells ml⁻¹ (PHA) or at 10⁶ cells ml⁻¹ (CD3/CD28) in RPMI–FBS complete with 50 U ml⁻¹ hIL-2 and challenged with lentiviral vectors for the assessment of single-cycle infectivity or with replication competent HIV-1 for spreading infection. Fresh media containing hIL-2 was replenished every 2–3 d.

Infectivity assay using single-cycle viruses. For human dendritic cells, 2.5 \times 10⁵ cells were seeded per well, in a 48-well plate, on the day of virus challenge. Media containing VSV G-pseudotyped lentiviral vector expressing GFP (HIV-1–GFP) was added to challenge cells in a total volume of 250 μ l. For human macrophages, 2.5 \times 10⁵ cells were seeded per well in a 24-well plate and challenged with HIV-1–GFP in a total volume of 500 μ l. The cells were also simultaneously challenged with HIV-1 VLPs, as indicated. A 1:50 volume of SIV–VLPs was also added to the medium during the virus challenge of dendritic cells or macrophages. To challenge human CD4⁺ cells activated with PHA, 5 \times 10⁵ cells were plated per well in a 96-well plate 3 d after the second PHA stimulation. For CD4⁺ cells stimulated with CD3/CD28 activator, 2 \times 10⁵ cells were plated in each well of a 96-well plate, 3 d after second stimulation. Cells were then challenged with GFP reporter viruses in a total volume of 200 μ l. For all three cell types, four dilutions of viral stocks, from 10⁵ to 10⁸ RTU ml⁻¹, were used to challenge cells. Where indicated, cells were pretreated with 8 μ M CsA, 8 μ M CsH or 2.5 μ M of non-immunosuppressive CypA inhibitors from Gilead (GS–CypA3 or GS–CypA48)³⁴, for 1 h before virus challenge. In experiments using CsH treatment, the media was replaced after 16 h of treatment to avoid CsH toxicity⁴⁴.

At 48 h post challenge with two-part HIV-1 vectors, or at 72 h post challenge with three-part lentiviral vectors, cells were harvested for flow cytometric analysis by pipetting (CD4⁺ T cells) or scraping (dendritic cells and macrophages). Cells were pelleted at 500g for 5 min and fixed in a 1:4 dilution of BD Cytofix Fixation Buffer with phosphate-buffered saline (PBS) without Ca²⁺ and Mg²⁺, supplemented with 2% FBS and 0.1% Na₃N.

Flow cytometry. Data were collected on an Accuri C6 (BD Biosciences) and plotted with FlowJo software v.10. Infectivity at each dilution, in each condition (CA mutant, CypA inhibitor or CypA knockdown) was compared to the infectivity of WT CA in the control condition. Dilutions yielding infectivity greater than 30% GFP⁺ cells were excluded from the analysis on the assumption that these were out of the linear range, according to the Poisson distribution.

Statistical analysis. Experimental *n* values and information regarding the statistical tests can be found in the figure legends. The data for infectivity assays using single-cycle viruses including at least three independent donors were statistically analysed using two-tailed paired *t*-tests compared to the control condition or the indicated condition for each donor. The qPCR data for experiments measuring viral cDNA levels with three biologically independent samples for each condition were analysed using two-tailed, unpaired *t*-tests for the comparison of two conditions as indicated in Fig. 2. The data from PLA quantification were assessed for statistical significance using two-tailed unpaired *t*-tests to compare two conditions as indicated in Fig. 4. All statistical analyses were performed using PRISM 8.2 (GraphPad Software).

qPCR for viral late reverse transcriptase product. Total DNA was extracted from cells using DNeasy Blood & Tissue Kit (Qiagen), following the manufacturer's instructions. Late reverse transcriptase products were detected with the TaqMan system using the primers pWPTS J1B fwd and pWPTS J2 rev with the late reverse transcription probe (LRT-P)⁴⁵. Mitochondrial DNA was used for normalization with the following primer/probe set: MH533, MH534 and Mito probe⁴⁶. The

primer and probe sequences are specified in Supplementary Table 3. The qPCR was performed in 20 µl reaction mix containing 1× TaqMan Gene Expression Master Mix (Applied Biosystems), 900 nM each primer, 250 nM TaqMan probe and 30 to 50 ng template DNA. After an initial incubation at 50 °C for 2 min and a second incubation at 95 °C for 10 min, 45 cycles of amplification were carried out at 95 °C for 15 s followed by 1 min and 30 s at 60 °C. Real-time PCR reactions were run on a CFX96 thermal cycler (Bio-Rad).

RT–qPCR. Total RNA was isolated in TRIzol reagent followed by RNA purification with RNeasy Plus Mini kit (Qiagen). First-strand cDNA was generated using SuperScript VILO Master Mix (Thermo Fisher) with random hexamers, in accordance with the manufacturer's instructions. Duplex qPCR was performed in 20 µl reaction mix containing 1× TaqMan Gene Expression Master Mix, 1× TaqMan Gene Expression Assay detecting TRIM5 (FAM dye-labelled, TaqMan probe ID no. Hs01552559_m1), 1× TaqMan Gene Expression Assay targeting a housekeeping gene OAZ1 (VIC dye-labelled, primer-limited, TaqMan probe ID no. Hs00427923_m1). Amplification was on a Bio-Rad CFX96 real-time PCR detection system, using 50 °C for 2 min, 95 °C for 10 min, then 45 cycles of 95 °C for 15 s and 60 °C for 60 s.

Western blot. Cells were lysed in Hypotonic Lysis Buffer: 20 mM Tris–HCl, pH 7.5, 150 mM NaCl, 10 mM EDTA, 0.5% NP-40, 0.1% Triton X-100 and complete mini protease inhibitor (Sigma-Aldrich) for 20 min on ice. The lysates were mixed 1:1 with 2× Laemmli buffer containing 1:20-diluted 2-mercaptoethanol, boiled for 10 min and centrifuged at 16,000g for 5 min at 4 °C. Samples were run on 4–20% SDS–PAGE and transferred to nitrocellulose membranes. Membrane blocking and antibody binding were in TBS Odyssey Blocking Buffer (Li-Cor). Primary antibodies used were rabbit anti-CypA (1:10,000 dilution; Enzo Life Sciences, catalogue no. BML-SA296) and mouse anti-β-actin (1:1,000 dilution; Abcam, catalogue no. ab3280). Goat anti-mouse-680 (Li-Cor, catalogue no. 925-68070) and goat anti-rabbit-800 (Li-Cor, catalogue no. 925-32211) as secondary antibodies were used at 1:10,000 dilutions. Blots were scanned on the Li-Cor Odyssey CLX.

PLA. 2.5 × 10⁵ macrophages were plated on 12 mm coverslips (Warner Instrument, catalogue no. CS-12R15) in 24-well plates. Cells were spinoculated at 1,200g using 6 × 10⁸ RT unit ml⁻¹ of three-part lentiviral vector (pALPS-GFP, p8.9 ΔNSB and pMD2.G, generated as above) at 13 °C for 2 h. The media was replaced with RPMI–HS complete containing 2 µM MG132 and either DMSO or 5 µM CsA; cells were incubated at 37 °C for 2 h. Coverslips were fixed with 3.7% formaldehyde (Thermo Fisher) in 0.1 M PIPES, pH 6.8, for 5 min at room temperature and then incubated at room temperature for 1 h in PBS containing 0.1% saponin, 10% donkey serum, 0.01% sodium azide, mouse anti-TRIM5α antibody (NIH AIDS Reagent Program, catalogue no. 12271) at a 1:750 dilution and rabbit anti-HIV-1 CA (p24) antibody (Abcam, catalogue no. ab32352) at a 1:400 dilution.

The samples were processed further using a Duolink In Situ Red kit (Sigma-Aldrich), following the instructions of the manufacturer. Next, samples were incubated with 10 µM phalloidin (fluorescein isothiocyanate; Enzo Life Science) and 1 mg ml⁻¹ Hoechst 33342 (Invitrogen), in PBS containing 10% donkey serum and 0.01% sodium azide for 30 min at room temperature.

Coverslips were mounted on slides and stored at –20 °C. Interaction was detected as fluorescent spots ($\lambda_{\text{excitation/emission}}$ at 598/634 nm). $\lambda_{\text{excitation/emission}}$ at 475/523 nm and $\lambda_{\text{excitation/emission}}$ at 390/435 nm were used to detect phalloidin and Hoechst, respectively. z-stack images were collected with a DeltaVision wide-field fluorescent microscope (Applied Precision, GE) and deconvolved with SoftWoRx deconvolution software v.7.0.0 (Applied Precision, GE). All images were acquired under identical acquisition conditions and analysed by Imaris 8.3.1 (Bitplane). Three-dimensional representations were constructed by using the Easy 3D function (Imaris 8.3.1).

Challenge with replication-competent HIV-1. 5 × 10⁵ macrophages per well in 12-well plates were challenged with 10⁸ RT units of HIV-1 for 2 h, in the presence of CsA or DMSO solvent, as indicated. Macrophage experiments used NL4-3_{MAC}; pNL4-3, in which *env* was replaced from the end of the signal peptide to the *env* stop codon, with macrophage-tropic *env* from GenBank (no. U63632.1). 3 d after secondary stimulation with CD3/CD28, 10⁶ CD4⁺ T cells per well in 48-well plates were challenged with 2 × 10⁷ RT units of HIV-1 for 2 h, in the presence of GS–CypA_{i3} or DMSO solvent, as indicated. CD4⁺ T cell experiments used HIV-1_{ZM249M}, a clade C transmission-founder strain. After HIV-1 challenge, cells were washed with fresh media and resuspended in 1 ml of RPMI–HS complete for macrophages or RPMI–FBS complete containing 50 U ml⁻¹ hIL-2 for CD4⁺ T cells. Where indicated, culture media also contained CsA, GS–CypA_{i3} or DMSO solvent. Every 2–3 d, culture supernatant was harvested to measure RT activity.

Reporting Summary. Further information on research design is available in the Nature Research Reporting Summary linked to this article.

Data availability

The plasmids described in Supplementary Table 1 are available at https://www.addgene.org/Jeremy_Luban/. All data generated or analysed during this study are presented in the Letter or Supplementary Information, or are available from the corresponding author on request.

Received: 4 April 2019; Accepted: 12 September 2019;
Published online: 21 October 2019

References

1. Yamashita, M. & Engelman, A. N. Capsid-dependent host factors in HIV-1 infection. *Trends Microbiol.* **25**, 741–755 (2017).
2. Luban, J., Bossolt, K. L., Franke, E. K., Kalpana, G. V. & Goff, S. P. Human immunodeficiency virus type 1 Gag protein binds to cyclophilins A and B. *Cell* **73**, 1067–1078 (1993).
3. Goldstone, D. C. et al. Structural and functional analysis of prehistoric lentiviruses uncovers an ancient molecular interface. *Cell Host Microbe* **8**, 248–259 (2010).
4. Malfavon-Borja, R., Wu, L. I., Emerman, M. & Malik, H. S. Birth, decay, and reconstruction of an ancient TRIMCyp gene fusion in primate genomes. *Proc. Natl Acad. Sci. USA* **110**, E583–E592 (2013).
5. Mu, D. et al. Independent birth of a novel TRIMCyp in *Tupaia belangeri* with a divergent function from its paralog TRIM5. *Mol. Biol. Evol.* **31**, 2985–2997 (2014).
6. Gilbert, C., Maxfield, D. G., Goodman, S. M. & Feschotte, C. Parallel germline infiltration of a lentivirus in two Malagasy lemurs. *PLoS Genet.* **5**, e1000425 (2009).
7. Katzourakis, A., Tristem, M., Pybus, O. G. & Gifford, R. J. Discovery and analysis of the first endogenous lentivirus. *Proc. Natl Acad. Sci. USA* **104**, 6261–6265 (2007).
8. Braaten, D., Franke, E. K. & Luban, J. Cyclophilin A is required for an early step in the life cycle of human immunodeficiency virus type 1 before the initiation of reverse transcription. *J. Virol.* **70**, 3551–3560 (1996).
9. Franke, E. K., Yuan, H. E. & Luban, J. Specific incorporation of cyclophilin A into HIV-1 virions. *Nature* **372**, 359–362 (1994).
10. Thali, M. et al. Functional association of cyclophilin A with HIV-1 virions. *Nature* **372**, 363–365 (1994).
11. Braaten, D. & Luban, J. Cyclophilin A regulates HIV-1 infectivity, as demonstrated by gene targeting in human T cells. *EMBO J.* **20**, 1300–1309 (2001).
12. Sokolskaja, E., Sayah, D. M. & Luban, J. Target cell cyclophilin A modulates human immunodeficiency virus type 1 infectivity. *J. Virol.* **78**, 12800–12808 (2004).
13. Towers, G. J. et al. Cyclophilin A modulates the sensitivity of HIV-1 to host restriction factors. *Nat. Med.* **9**, 1138–1143 (2003).
14. Berthou, L., Sebastian, S., Sokolskaja, E. & Luban, J. Cyclophilin A is required for TRIM5α-mediated resistance to HIV-1 in Old World monkey cells. *Proc. Natl Acad. Sci. USA* **102**, 14849–14853 (2005).
15. Sayah, D. M., Sokolskaja, E., Berthou, L. & Luban, J. Cyclophilin A retrotransposition into TRIM5 explains owl monkey resistance to HIV-1. *Nature* **430**, 569–573 (2004).
16. Luban, J. Cyclophilin A, TRIM5, and resistance to human immunodeficiency virus type 1 infection. *J. Virol.* **81**, 1054–1061 (2007).
17. Sayah, D. M. & Luban, J. Selection for loss of Ref1 activity in human cells releases human immunodeficiency virus type 1 from cyclophilin A dependence during infection. *J. Virol.* **78**, 12066–12070 (2004).
18. Sebastian, S. & Luban, J. TRIM5α selectively binds a restriction-sensitive retroviral capsid. *Retrovirology* **2**, 40 (2005).
19. Sebastian, S., Sokolskaja, E. & Luban, J. Arsenic counteracts human immunodeficiency virus type 1 restriction by various TRIM5 orthologues in a cell type-dependent manner. *J. Virol.* **80**, 2051–2054 (2006).
20. Stremmlau, M. et al. Specific recognition and accelerated uncoating of retroviral capsids by the TRIM5α restriction factor. *Proc. Natl Acad. Sci. USA* **103**, 5514–5519 (2006).
21. Stremmlau, M. et al. The cytoplasmic body component TRIM5α restricts HIV-1 infection in Old World monkeys. *Nature* **427**, 848–853 (2004).
22. Wilson, S. J. et al. Independent evolution of an antiviral TRIMCyp in rhesus macaques. *Proc. Natl Acad. Sci. USA* **105**, 3557–3562 (2008).
23. Virgin, C. A., Kratovac, Z., Bieniasz, P. D. & Hatzioannou, T. Independent genesis of chimeric TRIM5–cyclophilin proteins in two primate species. *Proc. Natl Acad. Sci. USA* **105**, 3563–3568 (2008).
24. Newman, R. M. et al. Evolution of a TRIM5–CypA splice isoform in old world monkeys. *PLoS Pathog.* **4**, e1000003 (2008).
25. Brennan, G., Kozyrev, Y. & Hu, S.-L. TRIMCyp expression in Old World primates *Macaca nemestrina* and *Macaca fascicularis*. *Proc. Natl Acad. Sci. USA* **105**, 3569–3574 (2008).
26. Boso, G. et al. Evolution of the rodent *Trim5* cluster is marked by divergent paralogous expansions and independent acquisitions of *TrimCyp* fusions. *Sci. Rep.* **9**, 11263 (2019).
27. Sokolskaja, E., Berthou, L. & Luban, J. Cyclophilin A and TRIM5α independently regulate human immunodeficiency virus type 1 infectivity in human cells. *J. Virol.* **80**, 2855–2862 (2006).
28. Pertel, T. et al. TRIM5 is an innate immune sensor for the retrovirus capsid lattice. *Nature* **472**, 361–365 (2011).

29. Fellmann, C. et al. An optimized microRNA backbone for effective single-copy RNAi. *Cell Rep.* **5**, 1704–1713 (2013).
30. McCauley, S. M. et al. Intron-containing RNA from the HIV-1 provirus activates type I interferon and inflammatory cytokines. *Nat. Commun.* **9**, 5305 (2018).
31. Yurkovetskiy, L. et al. Primate immunodeficiency virus proteins Vpx and Vpr counteract transcriptional repression of proviruses by the HUSH complex. *Nat. Microbiol.* **3**, 1354–1361 (2018).
32. Adachi, A. et al. Production of acquired immunodeficiency syndrome-associated retrovirus in human and nonhuman cells transfected with an infectious molecular clone. *J. Virol.* **59**, 284–291 (1986).
33. Salazar-Gonzalez, J. F. et al. Genetic identity, biological phenotype, and evolutionary pathways of transmitted/founder viruses in acute and early HIV-1 infection. *J. Exp. Med.* **206**, 1273–1289 (2009).
34. Mackman, R. L. et al. Discovery of a potent and orally bioavailable cyclophilin inhibitor derived from the sangliferrin macrocycle. *J. Med. Chem.* **61**, 9473–9499 (2018).
35. Husi, H. & Zurini, M. G. Comparative binding studies of cyclophilins to cyclosporin A and derivatives by fluorescence measurements. *Anal. Biochem.* **222**, 251–255 (1994).
36. Varshavsky, A. Ubiquitin fusion technique and related methods. *Methods Enzymol.* **399**, 777–799 (2005).
37. De Iaco, A. & Luban, J. Inhibition of HIV-1 infection by TNPO3 depletion is determined by capsid and detectable after viral cDNA enters the nucleus. *Retrovirology* **8**, 98 (2011).
38. Wu, X., Anderson, J. L., Campbell, E. M., Joseph, A. M. & Hope, T. J. Proteasome inhibitors uncouple rhesus TRIM5 restriction of HIV-1 reverse transcription and infection. *Proc. Natl Acad. Sci. USA* **103**, 7465–7470 (2006).
39. Colgan, J. et al. Cyclophilin A regulates TCR signal strength in CD4⁺ T cells via a proline-directed conformational switch in Itk. *Immunity* **21**, 189–201 (2004).
40. Bosco, D. A., Eisenmesser, E. Z., Pochapsky, S., Sundquist, W. I. & Kern, D. Catalysis of cis/trans isomerization in native HIV-1 capsid by human cyclophilin A. *Proc. Natl Acad. Sci. USA* **99**, 5247–5252 (2002).
41. Bock, M., Bishop, K. N., Towers, G. & Stoye, J. P. Use of a transient assay for studying the genetic determinants of Fv1 restriction. *J. Virol.* **74**, 7422–7430 (2000).
42. Laguette, N. et al. SAMHD1 is the dendritic- and myeloid-cell-specific HIV-1 restriction factor counteracted by Vpx. *Nature* **474**, 654–657 (2011).
43. Hrecka, K. et al. Vpx relieves inhibition of HIV-1 infection of macrophages mediated by the SAMHD1 protein. *Nature* **474**, 658–661 (2011).
44. Petrillo, C. et al. Cyclosporine H overcomes innate immune restrictions to improve lentiviral transduction and gene editing in human hematopoietic stem cells. *Cell Stem Cell* **23**, 820–832 (2018).
45. Reinhard, C., Bottinelli, D., Kim, B. & Luban, J. Vpx rescue of HIV-1 from the antiviral state in mature dendritic cells is independent of the intracellular deoxynucleotide concentration. *Retrovirology* **11**, 12 (2014).
46. Butler, S. L., Hansen, M. S. & Bushman, F. D. A quantitative assay for HIV DNA integration in vivo. *Nat. Med.* **7**, 631–634 (2001).

Acknowledgements

We thank T. Cihlar, B. Hahn, S. Hausmann, E. Hunter, R. Mackman, M. Pizzato and S. Yant for reagents. We are also grateful to anonymous blood donors who contributed leukocytes to this study. This work was supported by NIH grant nos. 5R01AI111809, 5DP1DA034990, 1R01AI117839 and 1R37AI147868 to J.L.

Author contributions

K.K. and J.L. designed the experiments. K.K. conducted and analysed most experiments. S.M.M., C.C. and W.E.D. cloned the plasmids used in this study. A.D., S.M.M., and L.Y. performed the HIV-1 spreading infections. S.K. acquired and analysed PLA samples. C.S.-D.-C. and E.M.C. provided advice and technical expertise for the imaging experiments. K.K. and J.L. wrote the manuscript with input from all authors.

Competing interests

The authors declare no competing interests.

Additional information

Extended data is available for this paper at <https://doi.org/10.1038/s41564-019-0592-5>.

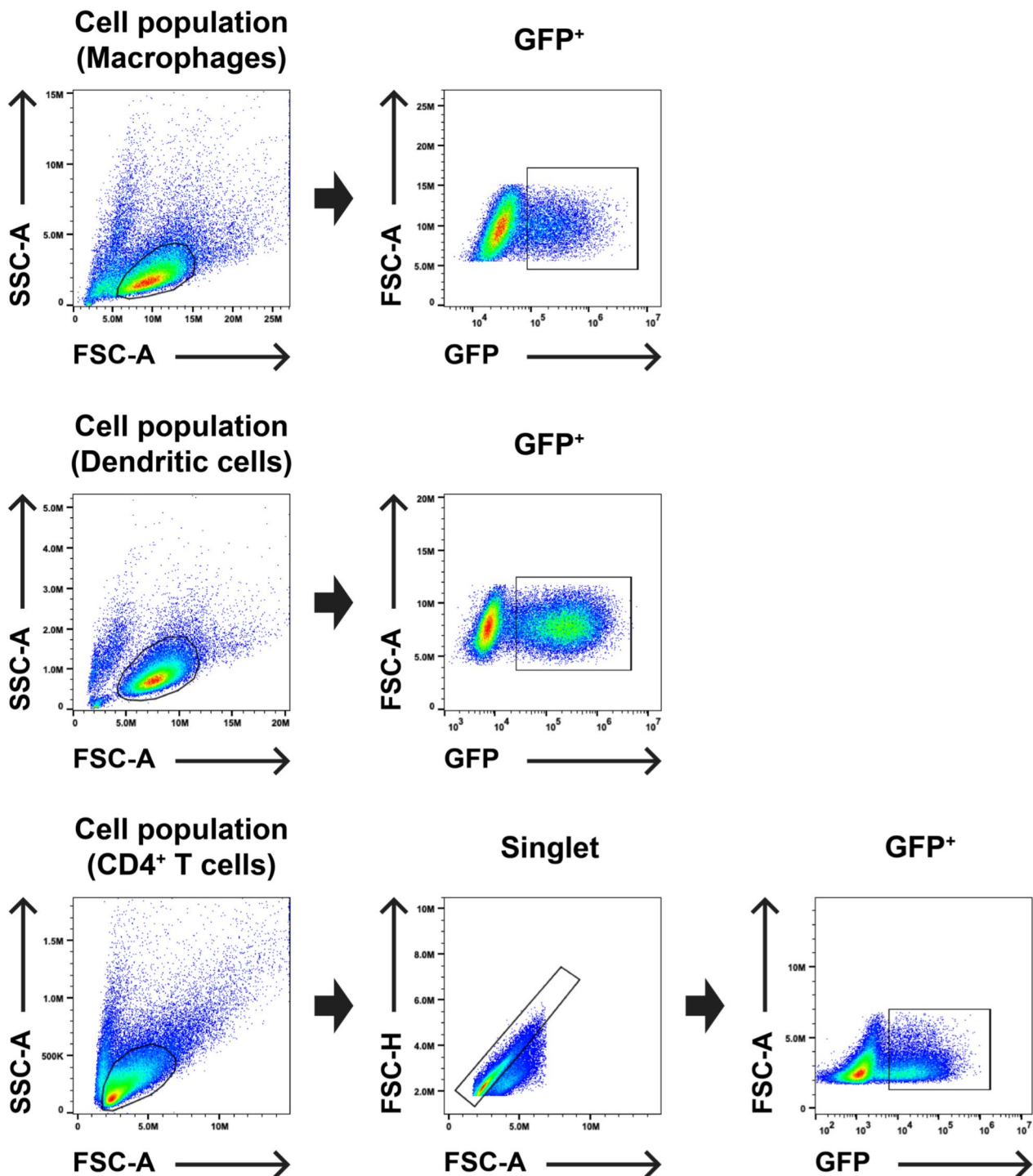
Supplementary information is available for this paper at <https://doi.org/10.1038/s41564-019-0592-5>.

Correspondence and requests for materials should be addressed to J.L.

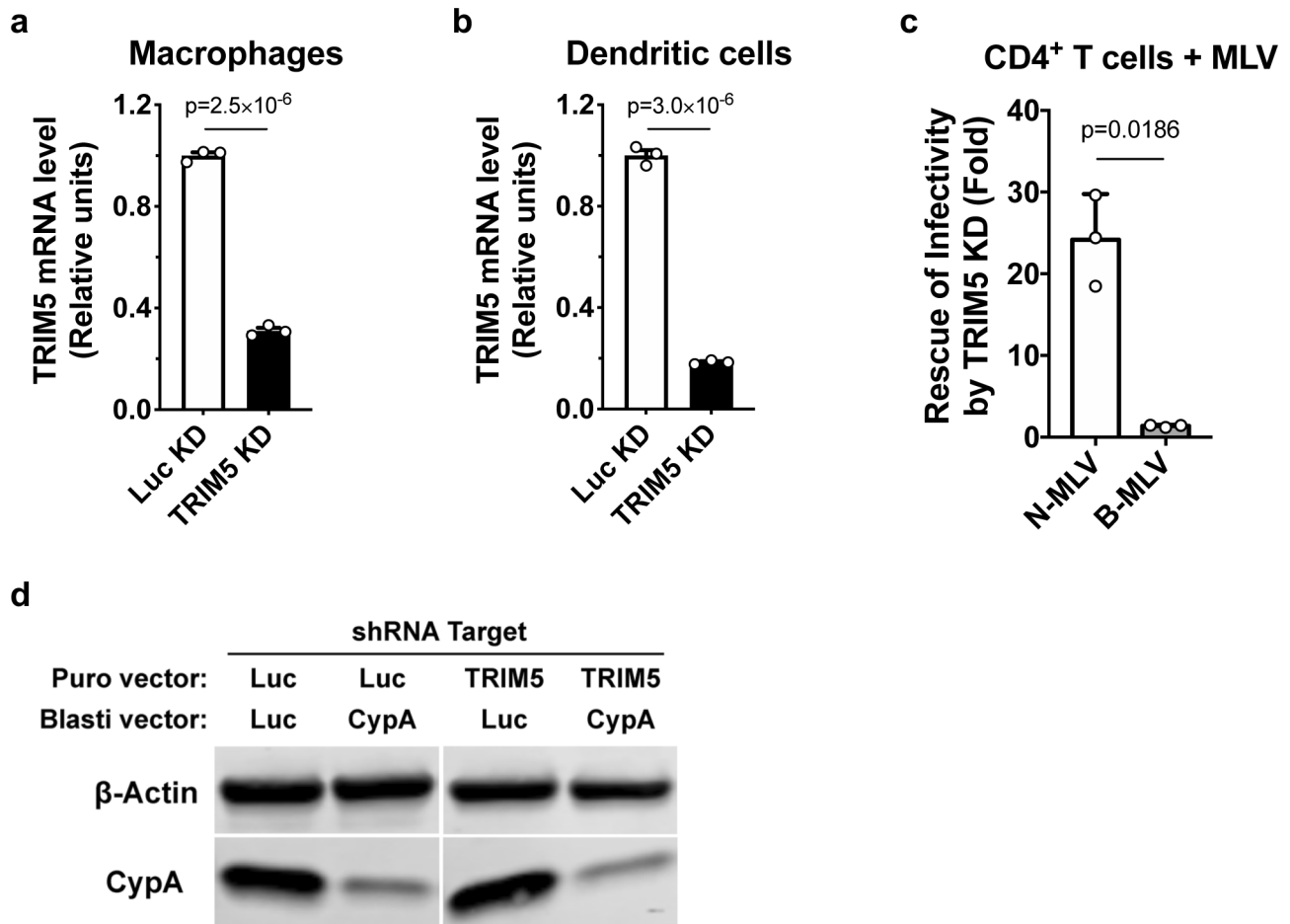
Reprints and permissions information is available at www.nature.com/reprints.

Publisher's note Springer Nature remains neutral with regard to jurisdictional claims in published maps and institutional affiliations.

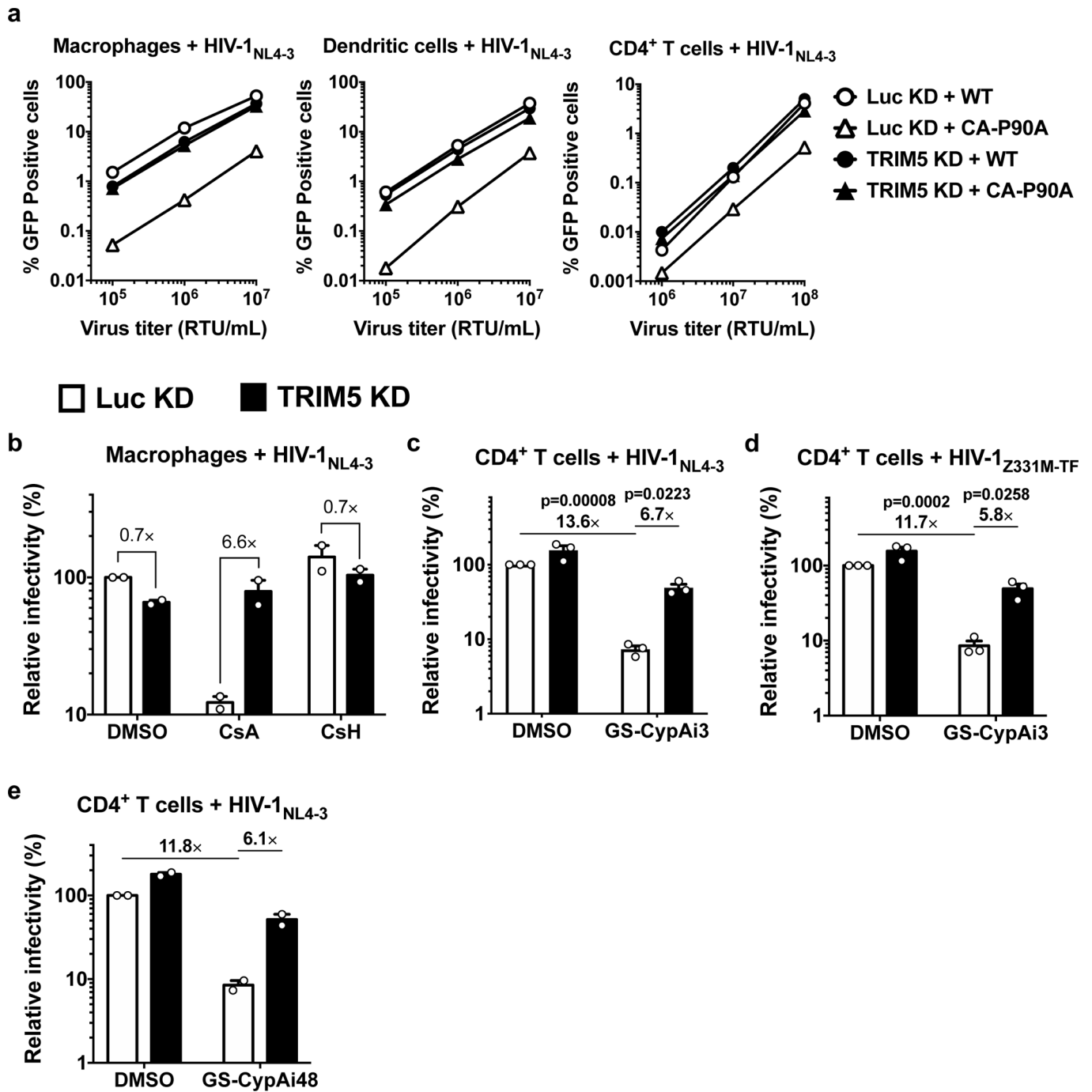
© The Author(s), under exclusive licence to Springer Nature Limited 2019



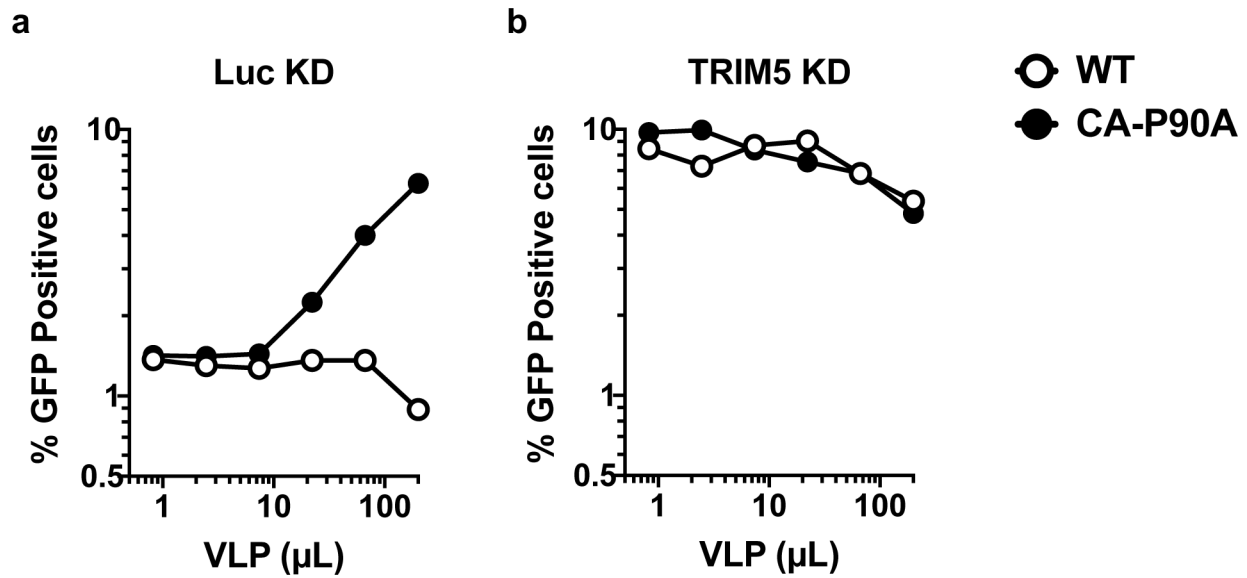
Extended Data Fig. 1 | Gating strategy for flow cytometry experiments assessing single cycle infectivity. Macrophage and dendritic cell populations, previously enriched as per the methods, were gated by SSC-A vs. FSC-A, as indicated, and then the GFP⁺ population was plotted vs. FSC-A. Enriched CD4⁺ T cells were gated by SSC-A vs. FSC-A, as indicated, then a singlet population was gated from FSC-H vs. FSC-A, and finally GFP⁺ cells were plotted vs. FSC-A.



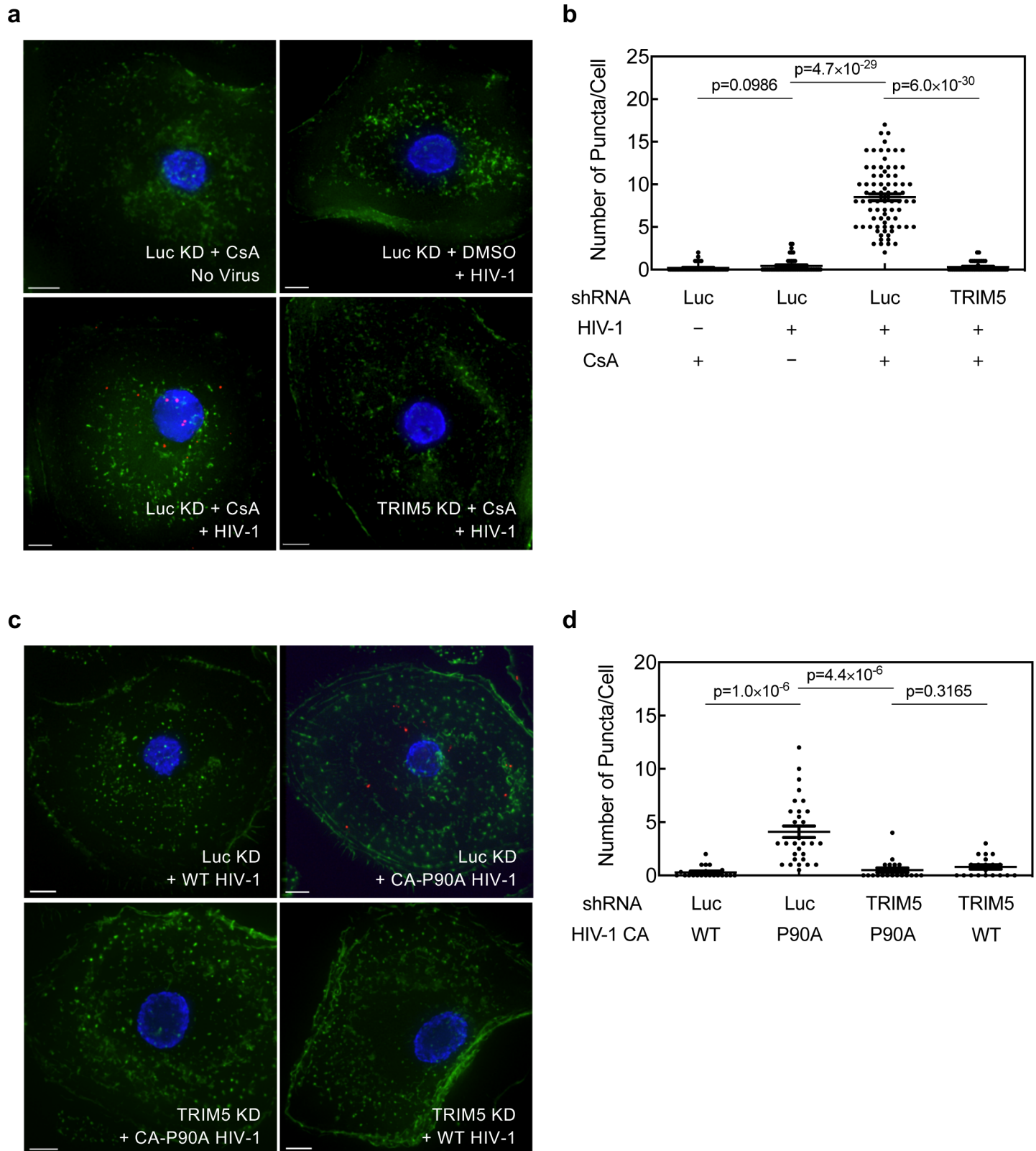
Extended Data Fig. 2 | Assessment of shRNA-mediated knockdown in primary human blood cells. a-c, Lentiviral vectors containing puromycin N- acetyltransferase (Puro^R) and shRNA targeting TRIM5 or Luc were used to transduce macrophages (**a**), dendritic cells (**b**), or CD4⁺ T cells (**c**). At 3 days post-transduction, cells were selected with puromycin for 3 days. Total RNA was isolated from the macrophages and dendritic cells, followed by cDNA synthesis, and qPCR with TaqMan detection of TRIM5 and the housekeeping gene OAZ1, for normalization (mean \pm SEM, $n=3$ independent samples). Significance was determined by two-tailed, unpaired t-test (**a** and **b**). The selected CD4⁺ T cells were challenged with N- or B-MLV vector harboring GFP reporter for 3 days. Flow cytometry was used to assess the percentage of GFP⁺ cells. The infectivity of each vector in TRIM5 knockdown cells was normalized to the Luc control condition. Shown is mean \pm SD ($n=3$ donors for each). Significance was determined by two-tailed, paired t-test (**c**). **d.** Macrophages were simultaneously transduced with two lentiviral vectors, the first expressing shRNA targeting TRIM5 or Luc with Puro^R, and the second expressing shRNA targeting CypA or Luc with blasticidin S-deaminase. After selection with both antibiotics, CypA and β -actin proteins were detected by western blot. Data shown is representative of three independent experiments using cells from three blood donors.



Extended Data Fig. 3 | CA-CypA interaction promotes HIV-1 transduction by inhibiting TRIM5 activity in primary human blood cells. **a**, Raw infectivity data for single cycle viruses, before normalization of infectivity to control condition. Shown are representative of three independent experiments using cells from three blood donors for each condition. **b**, Macrophages expressing shRNA targeting TRIM5 or Luc were challenged with single-cycle, VSV G-pseudotyped, HIV-1_{NL4-3}GFP in the presence of 8 μ M CsA, 8 μ M CsH, or DMSO solvent (mean \pm SEM, $n = 2$ donors). **c** and **d**, TRIM5 or Luc knockdown CD4⁺ T cells were challenged with single-cycle HIV-1_{NL4-3}GFP (**c**) or HIV-1_{Z331M-TF}GFP (**d**) in the presence of 2.5 μ M GS-CypAi3 or DMSO solvent alone (mean \pm SEM, $n = 3$ donors for each). **e**, HIV-1_{NL4-3}GFP was used to challenge TRIM5 or Luc knockdown CD4⁺ T cells with 2.5 μ M GS-CypAi48 or DMSO solvent alone (mean \pm SEM, $n = 2$ donors). Flow cytometry was used to measure the percentage of GFP⁺ cells, followed by normalization to WT in Luc knockdown cells. Significance was determined by two-tailed, paired t -test for data generated with at least three donors ($n = 3$).



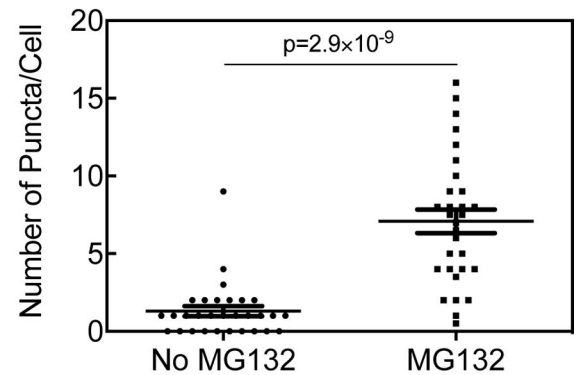
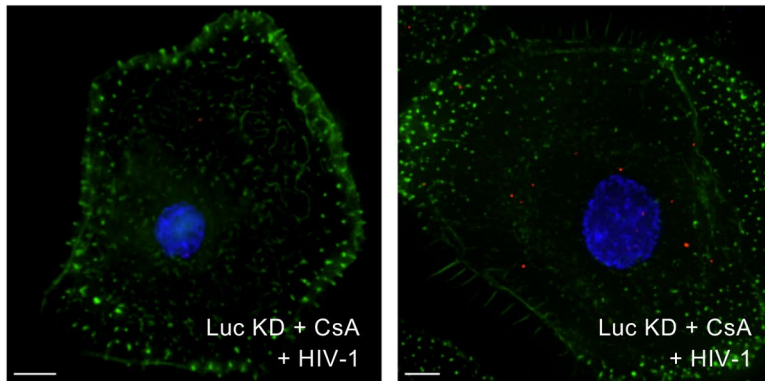
Extended Data Fig. 4 | Saturation of TRIM5 α -mediated restriction in primary human macrophages. Luc or TRIM5 knockdown macrophages were simultaneously challenged with a constant amount of single-cycle, VSV G-pseudotyped HIV-1_{NL4-3}GFP containing CA-P90A and the indicated quantities of HIV-1_{NL4-3} VLPs harboring either WT CA or CA-P90A. The percentage of GFP⁺ cells was assessed by flow cytometry at day 3 post-challenge. Data shown here are representative of four independent experiments performed on cells from four blood donors.



Extended Data Fig. 5 | CA-CypA interaction prevents association of endogenous TRIM5 α with HIV-1 CA in primary human macrophages. a-d, TRIM5 or Luc knockdown macrophages from a different blood donor than that used in Fig. 3 were challenged with VSV G-pseudotyped, HIV-1_{NL4-3}GFP in the presence of 5 μ M CsA or DMSO solvent for 2 hrs (**a** and **b**), or challenged with HIV-1_{NL4-3}GFP bearing WT CA or CA-P90A (**c** and **d**). PLA was then performed using anti-CA (p24) and anti-TRIM5 α antibodies. Representative images (**a** and **c**) show PLA puncta (red), nuclei stained with Hoechst (blue), and actin filaments stained with phalloidin (green). The plots (**b** and **d**) are the number of PLA puncta per cell in the PLA with mean \pm SEM. **b**, Luc KD + CsA No Virus, n=45 cells analyzed; Luc KD + DMSO + HIV-1, n=45; Luc KD + CsA + HIV-1, n=80; TRIM5 KD + CsA + HIV-1, n=45. **d**, Luc KD + WT HIV-1, n=20; Luc KD + CA-P90A HIV-1, n=30; TRIM5 KD + CA-P90A HIV-1, n=20; TRIM5 KD + WT HIV-1, n=20. Significance was determined by two-tailed, unpaired t-test. Scale bars in **a** and **c** are 5 μ m.

No MG132

+ MG132



Extended Data Fig. 6 | The effect of proteasome inhibitor treatment on the proximity ligation assay for HIV-1 CA and endogenous TRIM5 α . Luc control knockdown macrophages treated with 5 μ M CsA were challenged with VSV G-pseudotyped HIV-1_{NL4-3}GFP in the presence of 2 μ M MG132 or DMSO solvent. Cells were fixed and proximity ligation assay (PLA) was performed with anti-CA (p24) and anti-TRIM5 α antibodies. Representative images show PLA puncta (red), nuclei stained with Hoechst (blue), and actin filaments stained with phalloidin (green). Scale bars are 5 μ m. The graph on the right shows the number of puncta per cell in the PLA, after analysis of 30 cells per condition (mean \pm SEM). Significance was determined by two-tailed, unpaired t- test.

Reporting Summary

Nature Research wishes to improve the reproducibility of the work that we publish. This form provides structure for consistency and transparency in reporting. For further information on Nature Research policies, see [Authors & Referees](#) and the [Editorial Policy Checklist](#).

Statistics

For all statistical analyses, confirm that the following items are present in the figure legend, table legend, main text, or Methods section.

n/a Confirmed

- | | | |
|-------------------------------------|-------------------------------------|--|
| <input type="checkbox"/> | <input checked="" type="checkbox"/> | The exact sample size (n) for each experimental group/condition, given as a discrete number and unit of measurement |
| <input type="checkbox"/> | <input checked="" type="checkbox"/> | A statement on whether measurements were taken from distinct samples or whether the same sample was measured repeatedly |
| <input type="checkbox"/> | <input checked="" type="checkbox"/> | The statistical test(s) used AND whether they are one- or two-sided
<i>Only common tests should be described solely by name; describe more complex techniques in the Methods section.</i> |
| <input checked="" type="checkbox"/> | <input type="checkbox"/> | A description of all covariates tested |
| <input checked="" type="checkbox"/> | <input type="checkbox"/> | A description of any assumptions or corrections, such as tests of normality and adjustment for multiple comparisons |
| <input type="checkbox"/> | <input checked="" type="checkbox"/> | A full description of the statistical parameters including central tendency (e.g. means) or other basic estimates (e.g. regression coefficient) AND variation (e.g. standard deviation) or associated estimates of uncertainty (e.g. confidence intervals) |
| <input type="checkbox"/> | <input checked="" type="checkbox"/> | For null hypothesis testing, the test statistic (e.g. F , t , r) with confidence intervals, effect sizes, degrees of freedom and P value noted
<i>Give P values as exact values whenever suitable.</i> |
| <input checked="" type="checkbox"/> | <input type="checkbox"/> | For Bayesian analysis, information on the choice of priors and Markov chain Monte Carlo settings |
| <input checked="" type="checkbox"/> | <input type="checkbox"/> | For hierarchical and complex designs, identification of the appropriate level for tests and full reporting of outcomes |
| <input checked="" type="checkbox"/> | <input type="checkbox"/> | Estimates of effect sizes (e.g. Cohen's d , Pearson's r), indicating how they were calculated |

Our web collection on [statistics for biologists](#) contains articles on many of the points above.

Software and code

Policy information about [availability of computer code](#)

Data collection

BD Accuri C6 Software 1.0.264.21 was used to collect flow cytometry data.
Bio-Rad CFX Manager 3.1 software was used to collect quantitative PCR data.
Image Studio software 5.2 along with Li-Cor Odyssey CLx was used to collect western blot data.
SoftWoRx deconvolution software 7.0.0 (Applied Precision) along with DeltaVision wide-field fluorescent microscope was utilized to collect PLA imaging data.

Data analysis

FlowJo10 was utilized to analyze flow cytometry data.
Image Studio software 5.2 was used to analyze western blot data.
Imaris 8.3.1 software was used to analyze PLA imaging data.
GraphPad Prism 8 was used for all of graphical analysis.

For manuscripts utilizing custom algorithms or software that are central to the research but not yet described in published literature, software must be made available to editors/reviewers. We strongly encourage code deposition in a community repository (e.g. GitHub). See the Nature Research [guidelines for submitting code & software](#) for further information.

Data

Policy information about [availability of data](#)

All manuscripts must include a [data availability statement](#). This statement should provide the following information, where applicable:

- Accession codes, unique identifiers, or web links for publicly available datasets
- A list of figures that have associated raw data
- A description of any restrictions on data availability

All plasmids described in Supplementary Table 1, along with complete nucleotide sequences, are available at https://www.addgene.org/jeremy_luban/.

Field-specific reporting

Please select the one below that is the best fit for your research. If you are not sure, read the appropriate sections before making your selection.

Life sciences Behavioural & social sciences Ecological, evolutionary & environmental sciences

For a reference copy of the document with all sections, see [nature.com/documents/nr-reporting-summary-flat.pdf](https://www.nature.com/documents/nr-reporting-summary-flat.pdf)

Life sciences study design

All studies must disclose on these points even when the disclosure is negative.

Sample size	Pre-experiment, sample-size calculation was not performed, since effect size was unknown. In each case, experiments were performed using cells from at least three independent blood donors. The effects in our experiments were in fact large and reproducible, thus sample size calculation was not required.
Data exclusions	No data was excluded from analysis.
Replication	All experiments were performed with three technical replicates on at least three blood donors (biological replicates). Successful replication was confirmed.
Randomization	Randomization is not customary for standard molecular biology experiments such as these.
Blinding	For most experiments, investigators were not blinded to group allocation during data collection and analyses, since the results produce hard numbers with little need for interpretation. The outcomes in our experiments were clear, reproducible, and large in effect. The exception was the PLA assays, where the investigator who ran the microscopy software was blinded to the identity of the samples.

Reporting for specific materials, systems and methods

We require information from authors about some types of materials, experimental systems and methods used in many studies. Here, indicate whether each material, system or method listed is relevant to your study. If you are not sure if a list item applies to your research, read the appropriate section before selecting a response.

Materials & experimental systems

n/a	Involved in the study
<input type="checkbox"/>	<input checked="" type="checkbox"/> Antibodies
<input type="checkbox"/>	<input checked="" type="checkbox"/> Eukaryotic cell lines
<input checked="" type="checkbox"/>	<input type="checkbox"/> Palaeontology
<input checked="" type="checkbox"/>	<input type="checkbox"/> Animals and other organisms
<input checked="" type="checkbox"/>	<input type="checkbox"/> Human research participants
<input checked="" type="checkbox"/>	<input type="checkbox"/> Clinical data

Methods

n/a	Involved in the study
<input checked="" type="checkbox"/>	<input type="checkbox"/> ChIP-seq
<input type="checkbox"/>	<input checked="" type="checkbox"/> Flow cytometry
<input checked="" type="checkbox"/>	<input type="checkbox"/> MRI-based neuroimaging

Antibodies

Antibodies used

anti-CD14 antibody microbeads (Miltenyi, 130-050-201)
 anti-CD4 antibody microbeads (Miltenyi, 130-045-101)
 FITC-anti-CD3 (Biolegend, 317306, 1:100 dilution)
 APC-anti-CD4 (Biolegend, 317416, 1:100 dilution)
 anti-TRIM5alpha (NIH AIDS Reagent Program, 12271, 1:750 dilution)
 anti-p24 (Abcam, ab32352, 1:400 dilution)
 anti-Cyclophilin A (Enzo Life Sciences, BML-SA296, 1:10,000 dilution)
 anti-Actin (Abcam, ab3280, 1:1,000 dilution)
 anti-mouse-680 (Li-Cor, 925-68070, 1:10,000 dilution)
 anti-rabbit-800 (Li-Cor, 925-32211, 1:10,000 dilution)

Validation

All antibodies used in this study were validated by manufacturers and published papers. Anti-CD14 antibody microbeads and anti-CD4 antibody microbeads used for cell isolation by positive selection were validated by checking the surface markers of the isolated cells. FITC-anti-CD3 and APC-anti-CD4 were validated by staining the surface markers of cells having CD3 and CD4, or none, along with isotype control antibodies. Anti-Cyclophilin A was shown specific in our experiment by checking the protein expression in comparison to knockdown cells (Extended Data Fig. 2d). Anti-TRIM5alpha and Anti-p24 were also shown specific in our PLA imaging experiment by observing the fluorescent signals in comparison to knockdown cells or to cells without virus challenge (Fig. 3; Extended Data Fig. 5 and 6).

Eukaryotic cell lines

Policy information about [cell lines](#)

Cell line source(s)	HEK293 cells were acquired from ATCC.
Authentication	No authentication was performed for HEK293 cells.
Mycoplasma contamination	HEK293 cells tested negative for mycoplasma contamination by us.
Commonly misidentified lines (See ICLAC register)	None of the commonly misidentified cell lines were used in this study.

Flow Cytometry

Plots

Confirm that:

- The axis labels state the marker and fluorochrome used (e.g. CD4-FITC).
- The axis scales are clearly visible. Include numbers along axes only for bottom left plot of group (a 'group' is an analysis of identical markers).
- All plots are contour plots with outliers or pseudocolor plots.
- A numerical value for number of cells or percentage (with statistics) is provided.

Methodology

Sample preparation	Cells were fixed with BD CytoFix Fixation buffer prior to data acquisition on BD Accuri C6.
Instrument	BD Accuri C6
Software	BD Accuri C6 software 1.0.264.21 for data collection; FlowJo10 software for data analysis
Cell population abundance	Cell surface markers were used to confirm enrichment of the CD4+ T cells, macrophages, and dendritic cells
Gating strategy	Gating strategy for flow cytometry data is presented in the Supplementary Information.

Tick this box to confirm that a figure exemplifying the gating strategy is provided in the Supplementary Information.